Measuring the Higgs to Photon-Photon Branching Ratio at the Next Linear e^+e^- Collider. *

J. F. Gunion and P. C. Martin
Davis Institute for High Energy Physics, University of California, Davis CA, 95616

ABSTRACT

We examine the prospects for measuring the $\gamma\gamma$ branching ratio of a Standard-Model-like Higgs boson (h) at the Next Linear e^+e^- Collider when the Higgs boson is produced via W^+W^-–fusion: $e^+e^- \to \nu_e\bar{\nu}_e h$. In particular, we study the accuracy of such a measurement and the statistical significance of the associated signal as a function of the electromagnetic calorimeter resolution and the Higgs boson mass. We compare results for the W^+W^-–fusion production/measurement mode with the results obtained for the $e^+e^- \to Z^\star \to Zh$ production/measurement mode in a parallel earlier study.

I. INTRODUCTION

Discovery and study of Higgs boson(s) will be of primary importance at a Next Linear e^+e^- Collider (NLC). After discovery of a Higgs, the goal will be to determine as precisely as possible—independent of any model—its fundamental couplings and total width. Our concern is with a light Standard Model (SM) like Higgs boson which has a width too small for direct observation [1]. For such a Higgs boson, it will be necessary to determine $BR(h \to \gamma\gamma)$ in order to determine its total width and coupling constants. The procedure for ascertaining the Higgs total width and its $b\bar{b}$ partial width is outlined below. (Estimated errors given are summarized in Ref. [2].)

- Measure $\sigma(Zh)$ (in the missing mass mode) and $\sigma(Zh)BR(h \to b\bar{b})$ and compute:

$$BR(h \to b\bar{b}) = \frac{[\sigma(Zh)BR(h \to b\bar{b})]}{\sigma(Zh)} \; ; \qquad (1)$$

  the error in $BR(h \to b\bar{b})$ so obtained is estimated at $\pm 8\%$ to $\pm 10\%$.

- Measure at the associated $\gamma\gamma$ collider facility the rate for $\gamma\gamma \to h \to b\bar{b}$ (accuracy $\pm 5\%$) which is proportional to $\Gamma(h \to \gamma\gamma)BR(h \to b\bar{b})$ and compute (accuracy $\pm 11\%$ to $\pm 13\%$):

$$\Gamma(h \to \gamma\gamma) = \frac{[\Gamma(h \to \gamma\gamma)BR(h \to b\bar{b})]}{BR(h \to b\bar{b})} \; . \qquad (2)$$

- Measure in $e^+e^- \to \nu_e\overline{\nu}_e h$ (W^+W^-–fusion) the event rates for $h \to \gamma\gamma$ and $h \to b\bar{b}$. Then compute:

$$BR(h \to \gamma\gamma) = \frac{BR(h \to b\bar{b})[\sigma(\nu_e\bar{\nu}_e h)BR(h \to \gamma\gamma)]}{[\sigma(\nu_e\bar{\nu}_e h)BR(h \to b\bar{b})]} \; . \qquad (3)$$

- Finally, compute:

$$\Gamma_h^{\rm tot} = \frac{\Gamma(h \to \gamma\gamma)}{BR(h \to \gamma\gamma)} \; ; \;\; \Gamma(h \to b\bar{b}) = \Gamma_h^{\rm tot} BR(h \to b\bar{b}) \; . \qquad (4)$$

The above technique determines both $\Gamma_h^{\rm tot}$ and $\Gamma(h \to b\bar{b})$ in a model-independent way. This is desirable since knowledge of these fundamental Higgs properties is likely to be far more revealing than a simple measurement of $BR(h \to b\bar{b})$ alone. For example, in the minimal supersymmetric model (MSSM) parameters can be chosen such that the light Higgs, h^0, has total width and $b\bar{b}$ partial width that are both significantly different from the SM prediction, whereas the $b\bar{b}$ branching ratio is not. This occurs because the numerator and denominator, $\Gamma(h \to b\bar{b})$ and $\Gamma_h^{\rm tot}$, respectively, differ by similar amounts from the SM predictions, so that the ratio of the two changes only slightly. In general, interpretation of any branching ratio is ambiguous. We must be able to convert the measured branching ratios to the partial widths that are directly related to fundamental couplings. This is only possible if we can determine $\Gamma_h^{\rm tot}$ in a model-independent way.

Estimating the error in the determination of $BR(h \to \gamma\gamma)$ and how it propagates into errors in the determination of the total width and thence partial widths is very crucial. This is because the deviation of $BR(h \to \gamma\gamma)$ and the partial widths of a SM-like Higgs of an extended model from the predictions for the minimal SM Higgs boson may be small (as typical, for example, in the case of the h^0 of the MSSM when the pseudoscalar Higgs boson of the MSSM is heavy). It turns out that the dominant error in the partial width determinations will be that from the determination of $BR(h \to \gamma\gamma)$. Thus, it is vital that we determine the optimal procedures for minimizing the error in the latter.

Of course, deviations of $BR(h \to \gamma\gamma)$ itself from SM expectations could also be very revealing. In particular, by virtue of the fact that the coupling $h \to \gamma\gamma$ arises from charged loops, large deviations from SM predictions due to new particles (*e.g.* fourth generation, supersymmetry *etc.*) are possible. Regardless of the size of the deviations from SM predictions, determining $BR(h \to \gamma\gamma)$ at the NLC will be vital to understanding the nature of the Higgs boson and will provide an important probe of new physics that may lie beyond the SM.

II. SM SIGNAL AND BACKGROUND

In this report we examine expectations in the case of the Standard Model Higgs boson, h_{SM}. We focus on the mass range $50\,{\rm GeV} \lesssim m_{h_{SM}} \lesssim 150\,{\rm GeV}$ for which $BR(h_{SM} \to$

*Work supported in part by the Department of Energy and by the Davis Institute for High Energy Physics.

$\gamma\gamma$) is large enough to be potentially measurable. For the $e^+e^- \to \nu_e\overline{\nu}_e h_{SM}$ process that we are considering, the best rate is obtained by running the e^+e^- collider at the maximum possible energy. We adopt the canonical NLC benchmark energy of $\sqrt{s} = 500\,\mathrm{GeV}$.

Exact matrix elements are used for all calculations. For completeness, when calculating the signal (S) in the Xh_{SM} final state (where X is invisible), we include both production processes,

$$e^+e^- \to W^+W^-\nu_e\bar{\nu}_e \to \nu_e\bar{\nu}_e h_{SM}\,, \tag{5}$$

$$e^+e^- \to Z^\star \to Zh_{SM}\,, \tag{6}$$

with the subsequent decays:

$$h_{SM} \to \gamma\gamma \quad \text{and} \quad Z \to \nu_i\bar{\nu}_i \quad (i = e, \mu, \tau). \tag{7}$$

When calculating the background (B) we include all processes contributing to

$$e^+e^- \to \nu_i\bar{\nu}_i\gamma\gamma. \tag{8}$$

In our parallel study of the Zh_{SM} production/measurement mode, visible as well as invisible Z decays were included in both signal and background. [1]

III. CUTS AND CALORIMETRY CONSIDERATIONS

We compute both the signal and background rates for a small interval of the two-photon invariant mass, $\Delta m_{\gamma\gamma}(m_{h_{SM}})$, centered around $m_{h_{SM}}$.[2] The $\Delta m_{\gamma\gamma}$ interval will depend upon the resolution of the electromagnetic calorimeter (as we shall shortly discuss) and is adjusted in conjunction with other kinematic cuts so that the statistical error in measuring $\sigma(e^+e^- \to h_{SM}X)BR(h_{SM} \to \gamma\gamma)$, $\sqrt{S+B}/S$, is minimized. After exploring a wide variety of possible cuts, we found that the smallest error could be achieved using the following:

$$|y_{\gamma_1}| \le 2.0\,, \quad |y_{\gamma_2}| \le 2.0\,, \tag{9}$$

$$p_T^{\gamma_{1,2}} \ge p_T^{\gamma_{1,2}\ \min}(m_{h_{SM}})\,, \quad p_T^{\gamma_1} + p_T^{\gamma_2} \ge p_T^{\min}(m_{h_{SM}})\,, \tag{10}$$

$$M_{missing} = \sqrt{(p_{e^+} + p_{e^-} - p_{\gamma_1} - p_{\gamma_2})^2} \ge 130\,\mathrm{GeV}\,, \tag{11}$$

$$p_T^{\rm vis} = \sqrt{(p_x^{\gamma_1} + p_x^{\gamma_2})^2 + (p_y^{\gamma_1} + p_y^{\gamma_2})^2} \ge 10\,\mathrm{GeV}\,, \tag{12}$$

where $p_T^{\gamma_{1,2}}$ are the magnitudes of the transverse momenta of the two photons in the e^+e^- center-of-mass (by convention, $E_{\gamma_1} \ge E_{\gamma_2}$). The $M_{missing}$ cut effectively removes contributions from $e^+e^- \to Z^\star \to Zh_{SM}$ and the associated $e^+e^- \to Z\gamma\gamma \to \nu\overline{\nu}\gamma\gamma$ backgrounds. This is desirable because at $\sqrt{s} = 500\,\mathrm{GeV}$ the S/B ratio for these Z-pole-mediated processes is much smaller than that for the W^+W^-–fusion signal contribution and non-Z-pole backgrounds. Finally, the $p_T^{\rm vis}$ cut is used to eliminate contributions from events such as $e^+e^- \to e^+e^-\gamma\gamma$ where the e^+ and e^- are lost down the beam pipe leaving the signature of $\gamma\gamma$ plus missing energy [3].

Four different electromagnetic calorimeter resolutions are considered:

I: resolution like that of the CMS lead tungstate crystal [4] with $\Delta E/E = 2\%/\sqrt{E} \oplus 0.5\% \oplus 20\%/E$;

II: resolution of $\Delta E/E = 10\%/\sqrt{E} \oplus 1\%$;

III: resolution of $\Delta E/E = 12\%/\sqrt{E} \oplus 0.5\%$; and

IV: resolution of $\Delta E/E = 15\%/\sqrt{E} \oplus 1\%$.

Cases II and III are at the 'optimistic' end of current NLC detector designs [5]. Case IV is the current design specification for the JLC-1 detector [6]. For each resolution case, we have searched for the $p_T^{\gamma_1\ \min}$, $p_T^{\gamma_2\ \min}$, $p_T^{\min}$ and $\Delta m_{\gamma\gamma}$ values which minimize the error, $\sqrt{S+B}/S$, at a given Higgs boson mass. In Table I, we give these values as a function of Higgs mass m_h. Listed in Table II are the signal and background rates for the h_{SM} computed for these optimal choices. We assume that $m_{h_{SM}}$ will be known within $\Delta m_{h_{SM}} \ll \Delta m_{\gamma\gamma}$ and that the backgrounds can be accurately determined using data away from $m_{h_{SM}}$. All the results are for four years of running at $L = 50\ \mathrm{fb}^{-1}$ yearly integrated luminosity, *i.e.* a total of $L = 200\,\mathrm{fb}^{-1}$.

IV. RESULTS AND DISCUSSION

We present the statistical errors for measuring $\sigma BR(h_{SM} \to \gamma\gamma)$ in the W^+W^-–fusion measurement mode and compare with the results from our earlier, similar study of the Zh_{SM} production measurement mode [7]. We note that in the Zh_{SM} case the optimal results to be reviewed are only obtained by tuning the machine energy close to the value which maximizes the Zh_{SM} cross section for the given value of $m_{h_{SM}}$ and accumulating $L = 200\,\mathrm{fb}^{-1}$ at that energy. (The exact $\sqrt{s}$ values employed for the Zh_{SM} measurement mode and the associated cuts, the nature of which differ somewhat from the ones presented here for the fusion mode, are detailed in Ref. [7].) Since the optimal $\sqrt{s}$ for the Zh_{SM} mode is always substantially less than $500\,\mathrm{GeV}$, the devotion of so much luminosity to this single $\sqrt{s}$ value will only take place once the h_{SM} has already been discovered at the LHC or while running the NLC at $\sqrt{s} = 500\,\mathrm{GeV}$. If the NLC is first operated at $\sqrt{s} = 500\,\mathrm{GeV}$, either because a Higgs boson has not been detected previously or because other physics (*e.g.* production of supersymmetric particles) is deemed more important, data for measuring $\sigma BR(h_{SM} \to \gamma\gamma)$ using

[1] In this case, the Z-pole contributions to signal and background can be isolated for both visible and invisible final Z decays by requiring that the reconstructed 'Z' mass computed from the observed four-momenta of the photons and the incoming e^+ and e^- be near m_Z.

[2] The Higgs mass will be measured very precisely using the missing-mass technique in the Zh_{SM} mode.

the W^+W^-–fusion measurement mode will be accumulated. We will see that both the detector resolution and the actual value of $m_{h_{SM}}$ will enter into the decision regarding whether or not to devote luminosity to the Zh_{SM} measurement mode at a lower $\sqrt{s}$.

Figures 1-4 display plots of the statistical error, $\sqrt{S+B}/S$, and the statistical significance, $S/\sqrt{B}$, as functions of $m_{h_{SM}}$ for both $h_{SM} \to \gamma\gamma$ measurement modes. The following observations are useful:

- Figures 1 and 3 reveal that in resolution cases II-IV smaller errors are obtained in the Zh_{SM} measurement mode for a Higgs mass between $50\,\mathrm{GeV}$ and $120\,\mathrm{GeV}$, whereas the W^+W^- measurement mode yields smaller errors for $130 \lesssim m_{h_{SM}} \lesssim 150\,\mathrm{GeV}$. In resolution case I, the Zh_{SM} mode error is smaller for masses up to $130\,\mathrm{GeV}$.

- The absolute minimal statistical error (as obtained if we set $B=0$ and choose $\Delta m_{\gamma\gamma}$ large enough to accept the entire Higgs signal) for $50\,\mathrm{GeV} \lesssim m_{h_{SM}} \lesssim 150\,\mathrm{GeV}$ is:

  $\pm 8\%$ to $\pm 15\%$ in the Zh_{SM} measurement mode; and
  $\pm 15\%$ to $\pm 30\%$ in the W^+W^- measurement mode.

  These numbers indicate the extent to which the accuracy is limited simply as a result of the very small event rates in the $h_{SM} \to \gamma\gamma$ decay mode. The smaller error possible in the $B=0$ limit in the Zh_{SM} measurement mode is a result of the larger S values that can be achieved by running at the optimal $\sqrt{s}$.

- The smallest errors are obtained in the $90\,\mathrm{GeV} \lesssim m_{h_{SM}} \lesssim 130\,\mathrm{GeV}$. [3] In this region the statistical errors (including the computed background) for the best calorimeter resolution case (case I) are:

  $\pm 19\%$ to $\pm 22\%$ in the Zh_{SM} measurement mode;
  $\pm 22\%$ to $\pm 32\%$ in the W^+W^- measurement mode.

  For the worst resolution case (case IV) the errors are:

  $\pm 29\%$ to $\pm 35\%$ in the Zh_{SM} measurement mode;
  $\pm 26\%$ to $\pm 41\%$ in the W^+W^- measurement mode.

- Thus, if the detector does not have good electromagnetic calorimeter resolution, then the W^+W^-–fusion measurement mode is quite competitive with, and in some mass regions superior to, the Zh_{SM} measurement mode. However, if the smallest possible errors are the goal, excellent resolution is required and one must use the Zh_{SM} measurement mode techniques if $m_{h_{SM}} \lesssim 130\,\mathrm{GeV}$. The reasons behind these results are simple:

  - S/B tends to be substantial in the W^+W^-–fusion mode, implying relatively modest sensitivity to resolution, but S itself is limited (as noted earlier) so that even a $B=0$ measurement would not have a small error.
  - S is larger in the Zh_{SM} measurement technique (at the optimal $\sqrt{s}$ for the given $m_{h_{SM}}$ value) but B can only be made small enough for a big gain in $\sqrt{S+B}/S$ if the mass interval accepted can be kept small.

- The plots also reveal that in the lower mass region, $50 \lesssim m_{h_{SM}} \lesssim 80\,\mathrm{GeV}$, the error in the $\sigma BR(h_{SM} \to \gamma\gamma)$ measurement would be substantially lower in the Zh_{SM} mode, whereas in the upper mass region of $140 \lesssim m_{h_{SM}} \lesssim 150\,\mathrm{GeV}$ the errors are smaller in the W^+W^- measurement mode, especially if the resolution is not as excellent as assumed in case I.

Although observation of a clear Higgs signal in the $\gamma\gamma$ invariant mass distribution is not an absolute requirement (given that we will have observed the h_{SM} in other channels and will have determined its mass very accurately) it would be helpful in case there are significant systematics in measuring the $\gamma\gamma$ invariant mass. It is vital to be certain that $\Delta m_{\gamma\gamma}$ is centered on the mass region where the Higgs signal is present. Figures 2 and 4 show plots of the statistical significance, $S/\sqrt{B}$ *vs.* $m_{h_{SM}}$. They show that the mass regions for which $\geq 3\sigma$ measurements can be made depend significantly upon resolution.

- If excellent resolution (case I) is available then $S/\sqrt{B} \geq 3$ is achieved for $60\,\mathrm{GeV} \lesssim m_{h_{SM}} \lesssim 150\,\mathrm{GeV}$ in both the Zh_{SM} and W^+W^-–fusion measurement modes.

- If the resolution is poor (case IV) then $S/\sqrt{B} \geq 3$ is achieved for $90\,\mathrm{GeV} \lesssim m_{h_{SM}} \lesssim 130\,\mathrm{GeV}$ in the Zh_{SM} measurement mode and for $100\,\mathrm{GeV} \lesssim m_{h_{SM}} \lesssim 150\,\mathrm{GeV}$ in the W^+W^-–fusion mode.

We end this section by noting that the error in the determination of $BR(h_{SM} \to \gamma\gamma)$ is not precisely the same as the error in the $\sigma BR(h_{SM} \to \gamma\gamma)$ measurement. In the W^+W^-–fusion mode, Eq. (3) shows that errors in both $BR(h_{SM} \to b\bar{b})$ and $\sigma(\nu_e\bar{\nu}_e h_{SM})BR(h_{SM} \to b\bar{b})$ enter into the $BR(h_{SM} \to \gamma\gamma)$ error. The error in $BR(h_{SM} \to b\bar{b})$ will be about $\pm 8\% - \pm 10\%$. The error in $\sigma(\nu_e\bar{\nu}_e h_{SM})BR(h_{SM} \to b\bar{b})$ will probably be about $\pm 5\% - \pm 7\%$. These errors must be added in quadrature with the $\sigma(\nu_e\bar{\nu}_e h_{SM})BR(h_{SM} \to \gamma\gamma)$ error. In the Zh_{SM} measurement mode, $BR(h_{SM} \to \gamma\gamma)$ is computed as $\sigma(Zh_{SM})BR(h_{SM} \to \gamma\gamma)/\sigma(Zh_{SM})$. The $\sim \pm 7\%$ error in $\sigma(Zh_{SM})$ must be added in quadrature with the $\sigma(Zh_{SM})BR(h_{SM} \to \gamma\gamma)$ error. However, since the $\sigma BR(h_{SM} \to \gamma\gamma)$ errors in both the W^+W^--fusion and Zh_{SM} measurement modes are always $\gtrsim \pm 20\%$, quadrature additions of the magnitude summarized above will not be very significant. For example, for a σBR measurement of $\pm 20\%$ the quadrature additions would imply about $\pm 21\%$ ($\pm 22\%$) errors for $BR(h_{SM} \to \gamma\gamma)$ using the Zh_{SM} (W^+W^-–fusion) measurement mode procedures.

[3] This is the mass region predicted by the MSSM for the light Higgs, h^0.

V. CONCLUSIONS

We have studied the prospects for measuring $\sigma BR(h \to \gamma\gamma)$ for a SM-like Higgs boson at the NLC. The measurement will be challenging but of great importance. We have compared results for two different production/measurement modes: W^+W^-–fusion and Zh_{SM}. In the mass range of $90\,\mathrm{GeV}$ to $130\,\mathrm{GeV}$ where $BR(h_{SM} \to \gamma\gamma)$ is largest (a mass range that is also highly preferred for the light SM-like h^0 of the MSSM) the smallest errors in the measurement of $\sigma BR(h_{SM} \to \gamma\gamma)$ that can be achieved with an excellent CMS-style calorimeter (resolution case I) are $\gtrsim \pm 20\%$ using the Zh_{SM} measurement mode and $\gtrsim \pm 22\%$ using the W^+W^-–fusion measurement mode. For a calorimeter at the optimistic end of current plans for the NLC detector (cases II and III) the errors range from $\sim \pm 25\%$ to $\sim \pm 30\%$ for the Zh_{SM} mode and from $\sim \pm 26\%$ to $\sim \pm 41\%$ for the W^+W^-–fusion mode. The Zh_{SM} errors assume that the machine energy is tuned to the ($\leq 300\,\mathrm{GeV}$) $\sqrt{s}$ value which maximizes the Zh_{SM} event rate, and that $L = 200\ \mathrm{fb}^{-1}$ is accumulated there, whereas the W^+W^-–fusion errors assume that $L = 200\ \mathrm{fb}^{-1}$ is accumulated at $\sqrt{s} = 500\,\mathrm{GeV}$.

The desirability of running in the Zh_{SM} measurement mode can only be determined once the Higgs mass is known. To take full advantage of such running would require that the calorimeter be upgraded to a resolution approaching the CMS level of resolution. For resolution cases II or III and $m_{h_{SM}} \sim 120\,\mathrm{GeV}$, the accuracy of the measurement would be $\sim \pm 26\%$ in the W^+W^-–fusion measurement mode and $\sim \pm 25\%$ in the Zh_{SM} measurement mode, and there would be little point in running in the latter mode. For CMS resolution (case I), these respective errors become $\sim \pm 22\%$ and $\sim \pm 19\%$, a gain that is still somewhat marginal, especially given the fact that current estimates [8] are that the error on the $\sigma BR(h_{SM} \to \gamma\gamma)$ measurement at the LHC would be comparable, of order $\pm 22\%$ at $m_{h_{SM}} = 120\,\mathrm{GeV}$, so that statistics could be combined to give $\sim \pm 15\%$ for either NLC measurement mode. However, for smaller $m_{h_{SM}}$ values the LHC error will worsen significantly and the Zh_{SM} measurement mode becomes increasingly superior to the W^+W^-–fusion mode, especially if the calorimeter resolution is excellent. For Higgs masses above $m_{h_{SM}} \sim 120\,\mathrm{GeV}$, little would be gained by using the Zh_{SM} measurement mode; for the highest mass considered, $m_{h_{SM}} = 150\,\mathrm{GeV}$, using the Zh_{SM} mode would be disadvantageous.

Acknowledgements We thank J. Brau, R. Van Kooten, L. Poggioli and P. Rowson for helpful conversations.

VI. REFERENCES

[1] See J.F. Gunion, H.E. Haber, G.L. Kane and S. Dawson, *The Higgs Hunters Guide*, Addison-Wesley Publishing, and references therein.

[2] For a recent review, see J.F. Gunion, A. Stange, and S. Willenbrock, "Weakly-Coupled Higgs Bosons", in *Electroweak Symmetry Breaking and New Physics at the TeV Scale*, edited by T.L. Barklow, S. Dawson, H.E. Haber, and J.L. Siegrist (World Scientific, Singapore, 1996).

[3] C.-H. Chen, M.Drees, and J.F. Gunion, Phys. Rev. Lett. **76**, 2002 (1996).

[4] CMS Technical Proposal, CERN/LHCC 94-38 (1994).

[5] *Physics and Technology of the NLC*, BNL-52-502; Simulation homepage: http:// nlc.physics.upenn.edu /nlc /software /software.html.

[6] JLC-I, JLC Group, KEK Report 92-16, as summarized by K. Fujii, *Proceedings of the 2nd International Workshop on "Physics and Experiments with Linear e^+e^- Colliders"*, eds. F. Harris, S. Olsen, S. Pakvasa and X. Tata, Waikoloa, HI (1993), World Scientific Publishing, p. 782.

[7] J.F. Gunion, P.C. Martin, *Prospects for and Implications of Measuring the Higgs to Photon-Photon Branching Ratio at the Next Linear e^+e^- Collider*, preprint hep-ph/9607360.

[8] L. Poggioli, preliminary result obtained as part of the Light Higgs Working Group Study, Snowmass 1996.

Table I: For resolution choices I, II, III and IV, we tabulate $p_T^{\gamma_1\,\min}$, $p_T^{\gamma_2\,\min}$, $p_T^{\min}$, and $\Delta m_{\gamma\gamma}$ as a function of m_h (GeV).

m_h	$p_T^{\gamma_1\,\min}$	$p_T^{\gamma_2\,\min}$	$p_T^{\min}$	$\Delta m_{\gamma\gamma}^{I}$	$\Delta m_{\gamma\gamma}^{II}$	$\Delta m_{\gamma\gamma}^{III}$	$\Delta m_{\gamma\gamma}^{IV}$
50	30	10	40	0.7	2.0	2.1	2.3
60	30	10	60	1.0	2.2	2.3	2.7
70	30	20	65	1.1	2.4	2.7	3.2
80	30	20	70	1.3	2.7	2.7	3.6
90	30	20	70	1.4	3.1	3.1	4.1
100	40	20	75	1.8	3.4	3.4	4.5
110	40	20	85	2.0	4.2	4.2	5.0
120	40	20	95	2.2	4.6	4.6	5.4
130	50	20	100	2.3	4.9	4.7	5.9
140	50	30	110	2.5	5.3	4.8	6.3
150	50	30	120	2.4	5.4	5.1	6.8

Table II: For resolution choices I, II, III and IV, we tabulate S and B as a function of $m_{h_{SM}}$ (GeV) for $L = 200\ \mathrm{fb}^{-1}$.

$m_{h_{SM}}$	S_I	B_I	S_{II}	B_{II}	S_{III}	B_{III}	S_{IV}	B_{IV}
50	5.1	24	5.8	68	5.8	72	5.2	76
60	8.1	24	8.0	54	8.1	56	7.6	66
70	8.8	12	8.4	27	8.7	30	8.3	35
80	12	13	12	29	12	29	12	37
90	18	15	17	31	17	31	17	40
100	22	14	20	27	20	27	20	35
110	26	13	25	27	25	27	24	31
120	29	11	27	23	28	23	26	27
130	26	9.3	25	20	24	19	24	23
140	18	6.1	18	13	17	12	17	15
150	12	4.7	12	11	12	10	11	13

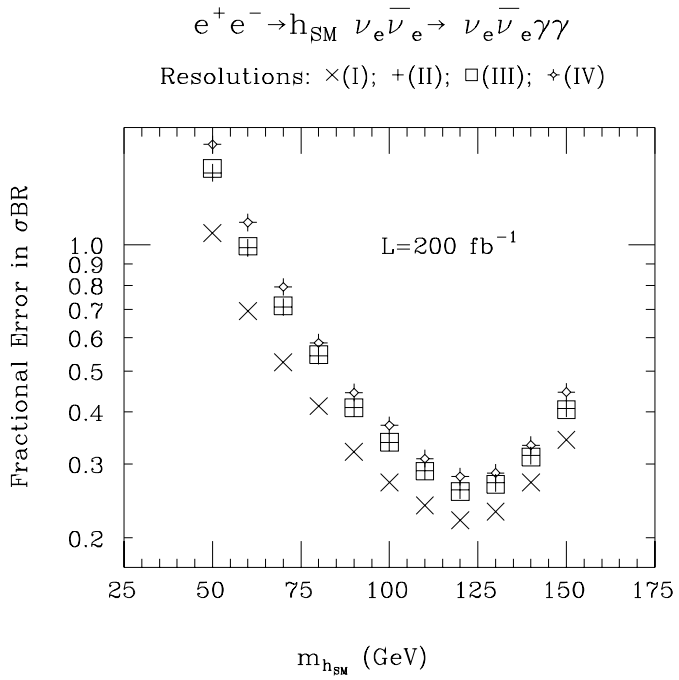

Figure 1: The fractional error in the measurement of $\sigma(\nu_e\bar{\nu}_e h_{SM})qBR(h_{SM} \to \gamma\gamma)$ as a function of $m_{h_{SM}}$.

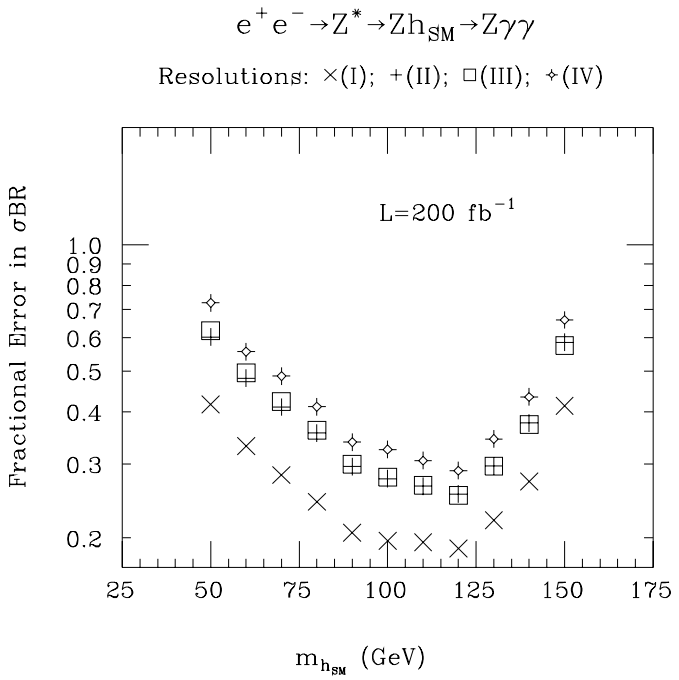

Figure 3: The fractional error in the measurement of $\sigma(Zh_{SM})BR(h_{SM} \to \gamma\gamma)$ as a function of $m_{h_{SM}}$.

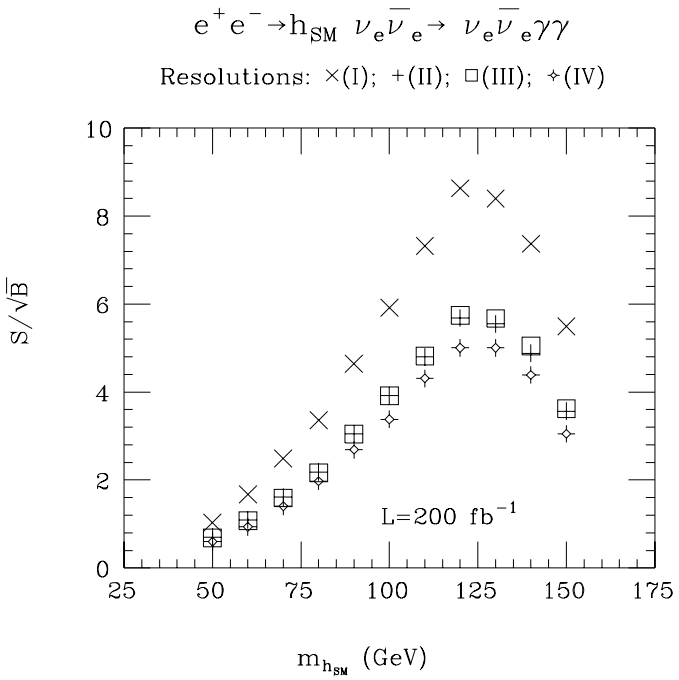

Figure 2: Results for $S/\sqrt{B}$ in the W^+W^-–fusion production mode at $L = 200\ \mathrm{fb}^{-1}$ as a function of $m_{h_{SM}}$.

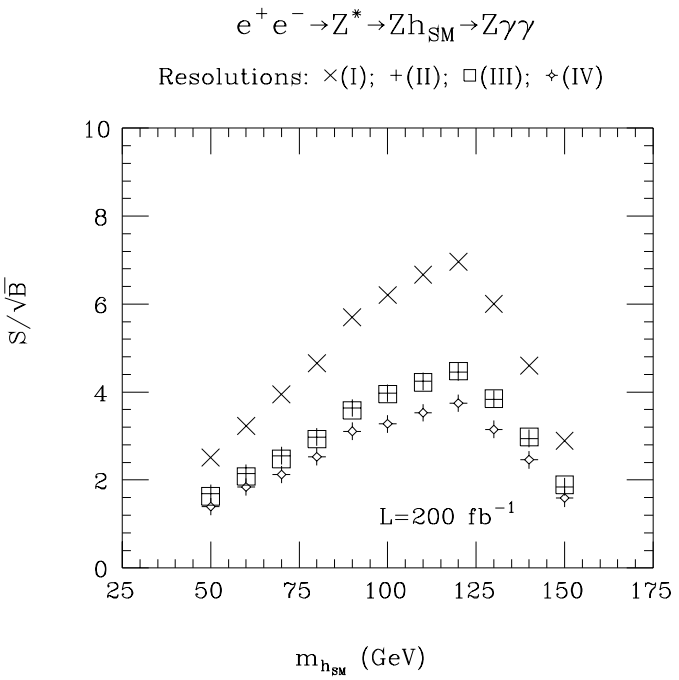

Figure 4: Results for $S/\sqrt{B}$ in the Zh_{SM} production mode at $L = 200\ \mathrm{fb}^{-1}$ as a function of $m_{h_{SM}}$.